International Journal of Zoology and Applied Biosciences ISSN: 2455-9571
Volume 11, Issue 5, pp: 265-273, 2026
https://doi.org/10.55126/ijzab.2026.v11.i05.033 http://www.ijzab.com

Research Article

GREEN SYNTHESIS AND CHARACTERIZATION OF *BREYNIA RETUSA* MEDIATED SILVER NANOPARTICLES AND THEIR I*N VITRO* ANTIUROLITHIATIC ACTIVITY AGAINST STRUVITE CRYSTALS

[1]Mullai Nila K, [2]Priya G and [3*]Chanthuru A

[1]Department of Microbiology and Biotechnology, Bharath Institute of Higher Education and Research, Chennai. Tamil Nadu, India.
[2]Department of Biochemistry, Mohamed Sathak College of Arts and Science, Sholinganallur, Chennai. Tamil Nadu, India.
[3]Department of Microbiology, EGS Pillay Arts and Science College, Nagapattinam, Tamil Nadu, India.

Article History: Received 8th June 2026; Accepted 17th August 2026; Published 30th September 2026

ABSTRACT

Urolithiasis remains a significant clinical challenge, necessitating eco-friendly therapeutic approaches. This study investigates the green synthesis of silver nanoparticles (AgNPs) using ethanolic stem extract of *Breynia retusa* and evaluates their antiurolithiatic potential. Phytochemical screening revealed abundant bioactive compounds, with tannin (0.128 mg/g) and phenol (0.02 mg/g) as dominant constituents. AgNPs were synthesized via reduction of $AgNO_3$, confirmed by a surface plasmon resonance peak at 467 nm. Characterization using FTIR, XRD, SEM, and EDX indicated crystalline, spherical nanoparticles with sizes ranging from 72-90 nm and silver content of 64.81%. In vitro struvite crystal growth inhibition was assessed using a gel diffusion method. The highest inhibition (89.8%) was observed at 5% AgNP concentration, significantly reducing crystal mass from 2.46 g (control) to 0.25 g. These findings demonstrate that B. retusa-mediated AgNPs exhibit potent antiurolithiatic activity and offer a promising, sustainable alternative for kidney stone management.

Keywords: Urolithiasis, *Breynia retusa,* FTIR, XRD, SEM, EDX.

INTRODUCTION

Urolithiasis remains a major global health concern, necessitating the development of safer and eco-friendly therapeutic approaches. It is a multifactorial disorder characterized by the formation of calculi within the urinary tract, affecting approximately 10-15% of the population worldwide and exhibiting a high rate of recurrence (Alelign & Petros, 2018; Stamatelou *et al*., 2003). The process of stone formation involves a series of physicochemical events including supersaturation of urine, nucleation, crystal growth, aggregation, and retention within the renal system. Among the different types of urinary stones, struvite (magnesium ammonium phosphate) crystals are frequently associated with urinary tract infections and are known for their rapid formation and recurrence (Hesse *et al*., 2003). Conventional treatment strategies such as extracorporeal shock wave lithotripsy (ESWL), ureteroscopy, and surgical removal are commonly employed; however, these methods are often associated with high cost, recurrence, and potential complications (Johri *et al*., 2010). These limitations have led to increased interest in alternative therapies, particularly plant-based medicines, which are considered safer and more economical. Medicinal plants are rich sources of bioactive compounds such as flavonoids, tannins, phenolics, alkaloids, and terpenoids, which are known to inhibit various stages of stone formation, including nucleation, growth, and aggregation (Pareta *et al*., 2012; Bashir & Gilani, 2009; Nagarajan *et al.,* 2019).

In recent years, green nanotechnology has emerged as an innovative approach that integrates plant-based therapeutics with nanoscience. The synthesis of silver nanoparticles (AgNPs) using plant extracts offers advantages such as eco-friendliness, cost-effectiveness, and enhanced biological activity. Plant-mediated AgNPs have been reported to exhibit significant antimicrobial, antioxidant, and

*Corresponding Author: Mr. Chanthuru A, Department of Microbiology, EGS Pillay Arts and Science College, Nagapattinam, Tamil Nadu, India., Email: chanthuru.microbiotech@gmail.com

therapeutic properties, making them promising candidates in biomedical applications (Gurunathan *et al.,* 2015; Li *et al.,* 2010). Breynia retusa, a small deciduous shrub belonging to the family Phyllanthaceae, is widely distributed in tropical regions and has been traditionally used for treating various ailments, including urinary disorders. The plant is characterized by slender branches and small elliptic leaves and is known to contain diverse phytoconstituents such as flavonoids, tannins, phenolics, and alkaloids. These compounds are associated with antioxidant and anti-inflammatory properties, which play a crucial role in preventing oxidative stress-induced crystal formation (Pareta *et al*., 2012). Therefore, the present study focuses on the green synthesis of silver nanoparticles using the ethanolic stem extract of *Breynia retusa* and evaluates there *in vitro* antiurolithiatic activity against struvite crystal formation, aiming to provide a sustainable and effective alternative for kidney stone management.

MATERIALS AND METHODS

The present study was designed to evaluate the antiurolithiatic activity of plant-mediated silver nanoparticles through *in vitro* experimentation. All chemicals and reagents used in the study were of analytical grade, and double-distilled water was used throughout the experimental procedures.

Collection and Preparation of Plant Material

Fresh stems of the *Breynia retusa* were collected from a local area and authenticated by a qualified botanist. The plant material was thoroughly washed with tap water followed by distilled water to remove dust and impurities. It was then shade dried at room temperature for several days until complete moisture removal. The dried material was coarsely powdered using a mechanical grinder and stored in an airtight container for further use.

Preparation of Plant Extract

Approximately 10 g of powdered plant material was extracted with 100 mL of ethanol using a Soxhlet apparatus for 6-8 hours. The extract was filtered using Whatman No.1 filter paper and concentrated under reduced pressure using a rotary evaporator. The obtained crude extract was stored at 4°C for further experimental analysis.

Phytochemical Analysis

Preliminary qualitative phytochemical screening of the extract was carried out to identify the presence of bioactive constituents such as alkaloids, flavonoids, tannins, phenols, terpenoids, and saponins using standard protocols. Quantitative estimation of selected phytoconstituents was also performed using spectrophotometric methods.

Green Synthesis of Silver Nanoparticles

Silver nanoparticles were synthesized by adding 10 mL of plant extract to 90 mL of 1 mM aqueous silver nitrate ($AgNO_3$) solution. The reaction mixture was incubated at room temperature under dark conditions to prevent photoreduction. A visible color change from pale yellow to brown indicated the formation of silver nanoparticles. The solution was centrifuged at 10,000 rpm for 15 minutes, and the pellet obtained was washed repeatedly with distilled water and dried for further characterization.

Characterization of Silver Nanoparticles

The synthesized nanoparticles were characterized using various analytical techniques. UV-Visible spectroscopy was used to confirm nanoparticle formation by observing surface plasmon resonance peaks. Fourier Transform Infrared (FTIR) spectroscopy was performed to identify functional groups involved in reduction and stabilization. X-ray diffraction (XRD) analysis determined the crystalline nature of nanoparticles, while scanning electron microscopy (SEM) provided information on morphology and size. Energy dispersive X-ray (EDX) analysis confirmed elemental composition.

In Vitro Antiurolithiatic Activity

The antiurolithiatic activity was evaluated using a single diffusion gel growth technique (Nagarajan et al., 2019). Sodium metasilicate solution was prepared and adjusted to appropriate pH, followed by the addition of ammonium dihydrogen phosphate to form a gel medium. Magnesium acetate solution was carefully layered over the gel. Different concentrations of plant extract and synthesized nanoparticles (0.15%, 0.25%, 0.50%, 0.75%, and 1.0%) were introduced into the system. A control without extract was also maintained. The setup was incubated at room temperature for several days to allow crystal formation. The growth of struvite crystals was monitored periodically, and crystal size was measured using a calibrated scale. The percentage inhibition of crystal growth was calculated by comparing treated samples with the control.

Statistical Analysis

All experiments were conducted in triplicate, and the results were expressed as mean ± standard deviation. Statistical significance was analyzed using appropriate methods to validate the reproducibility and reliability of the results.

RESULTS AND DISCUSSION

The phytochemical constituent presents in ethanolic extract of *Breynia retusa* stem to make of use various tests quality shown in Table 1. It shows that the ethanolic extract of *Breynia retusa* stem reveal the presence of terpenoid, flavanoid, tannin, alkaloids, steroids, coumarin, emodin, anthroquinone, xanthoproteins, phenol, saponin, glycosides, phlobatannins, anthocyanin, carbohydrate, lawanthocyanin, cardicglycosides these are all have medicinal and physiological activities. The phytochemical consists screening the quantitative analysis of *Hybanthus enneaspermus* bark extract was various amount have been reported. The higher quantity present in bark extract is saponin followed by tannin, phenol, flavonoids, terpenoids, and alkaloids show the table 2. The weighed 5mg of plant extract to the 50ml of 3mM silver nitrate. The mixture is set to react in an environmental condition and silver get reduced as Ag+ ion. After few minutes the colour changes are observed. The colour changes from a transparent white to dark brown. This shows the formation of silver nanoparticles. The formation of silver nanoparticle that is Ag+ ion was confirmed by the UV- spectral analysis (Figure 1).

Table 1. Qualitative analysis of ethanolic extract of *Breynia retusa* stem.

S. No	Test	Observation	Result
1	Terpenoid	Reddish brown	+++
2	Flavanoid	Yellow colour	+++
3	Saponin	Blue colour	+++
4	Tannin	Brownish green	+++
5	Alkaloids	Yellow collour	+++
6	Steroids	Reddish brown	+++
7	Glycosides	Violet, blue	+++
8	Phlobatanins	Red precipitate	+++
9	Protein	White	++
10	Coumarin	Yellow	+++
11	Emodin	Red	+++
12	Anthroquinone	Pink, Violet	+++
13	Anthocyanin	Pinkish red, Blusih violet	+++
14	Carbohydrate	Reddish pink	++
15	Lanthocyanin	Red	+++
16	Cardiacglycosides	Brown ring / Violet	++
17	Xanthoproteins	Blue /black	+++
18	Phenol	Reddish / orange	+++

+ - Trace ++ - Moderate +++ - Strong A - Absent

Table 2. Quantitative analysis of ethanolicextract of *Breynia retusa* stem.

S. No	Phytoconstitutents	Quantity (mg/g)
1	Saponin	0.022
2	Alkaloids	0.014
3	Flavonoids	0.009
4	Phenol	0.02
5	Terpenoids	0.014
6	Tannin	0.128

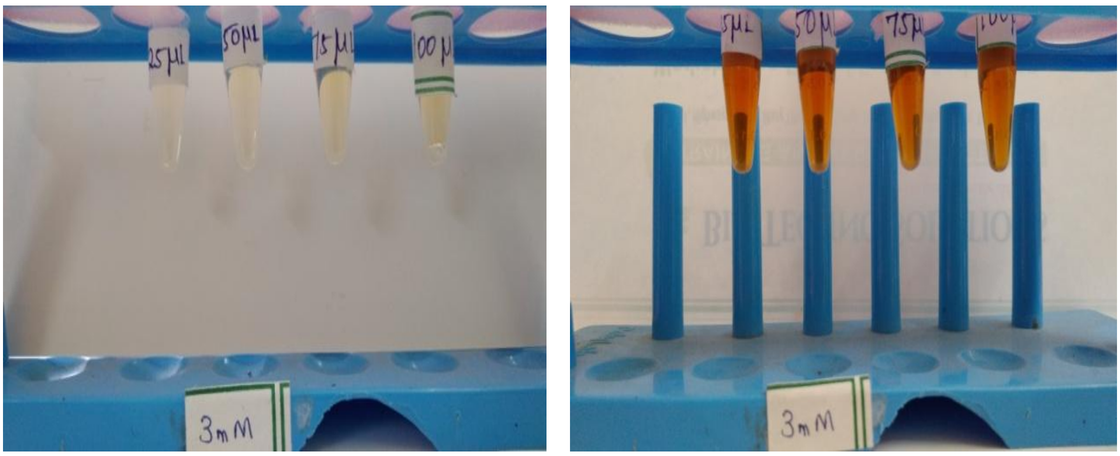

Figure 1. Before and after synthesize of silver nanoparticles.

In this experiment, addition of sample in to the glass vial containing $AgNO_3$ led to the change in color from colorless to reddish brown indicates the presence of silver nanoparticles. Plasma resonance band was observed by UV spectra at the range of 467 nm (Figure 2). The FT-IR spectrum of extract gives details about the functional group involved in the silver ions reduction. The FT-IR spectra of synthesized silver nanoparticles are shown in Figure 3. The corresponding peaks observed in the synthesized silver Nanoparticles are shown in the table 3. The XRD spectrum was recorded to confirm the crystalline structure of synthesized AgNPs using sample. The diffraction peaks were obtained by root-AgNPs is observed at 37.45, 45.34, 67.55 and 78.12 in the 2Θ range (Figure 4). The peaks can be indexed to the (111), (200), (220) and (311) reflection of face centered cubic structure of metallic silver which suitably matched the standard diffraction data with those reported for silver by joint committee on powder diffraction standards (JCPDS) FILE NO :040783.

The SEM image is employed to predict the size and morphology of resultant silver nanoparticles using sample. The size (diameter) of the nanoparticles lie between 72.74-90.97 nm regions (Figure 5) the average size of the nanoparticles is ~ 200 nm, whereas the shapes were spherical and cubic. From the previous studies suggested that the SEM analysis it was found that leaves of *Euphorbia hirta* silver nanoparticles have spherical shape and the average size is 13-61 nm[25]. Energy dispersive X-ray (EDX) spectrometer analysis confirmed the elemental signal of silver nanoparticles. The Y-axis (vertical) represents the number of X-ray counts while X-axis (horizontal) shows the energy in KeV. EDX spectrum recorded for the silver nanoparticles was shown in Fig. 6 with additional peak of oxygen because of biomolecules attached to the silver nanoparticles surface. From EDX spectra, it is found that silver nanoparticles are reduced by *Brenia retusa* have the silver weight percentage as 64.81% (Table 4).

The crystallization and nucleation characteristics of effect of *Breynia retusa stem* in struvite crystals is determined by evaluating the formed crystal weight (Table 5). The crystal growth is developed by gel method. The gel method consists the control using the magnesium acetate results shows the high yield of crystal growth. The nucleation takes place within 24 hours. Followed by add the synthesized silver nanoparticles of *Breynia retusa stem* (supernatant solution). After the nucleation, the addition of synthesized Ag+ nanoparticles the reduced masses and delayed nucleation of crystal observe within 96 hours (Figure 7,8 &9).

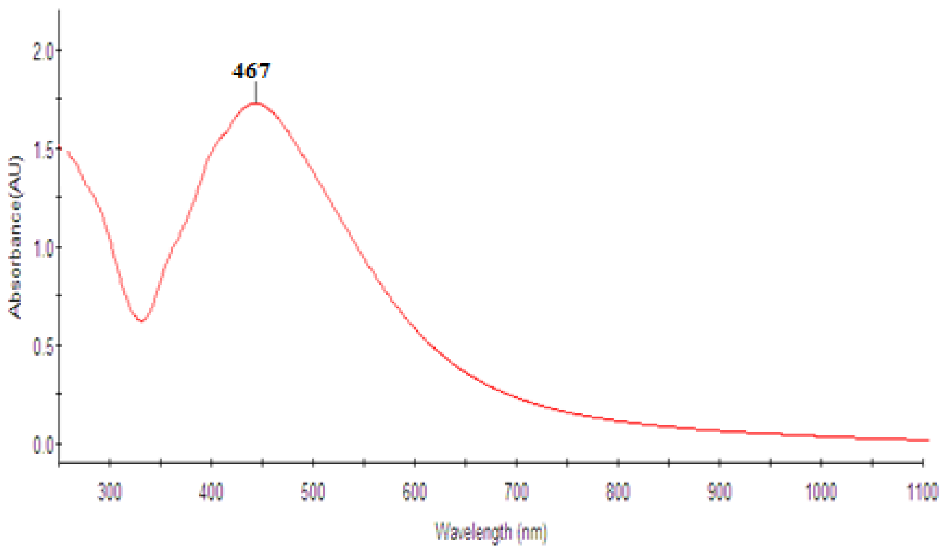

Figure 2. UV-Vis spectrum of synthesized silver nanoparticles using sample.

Table 3. FTIR band values of synthesized silver nanoparticles.

Functional group	Band	Frequency, cm^{-1}
Primary amine	medium band	3435cm^{-1} corresponds to N-H stretching vibrations
Isothiocyanate	strong band	2075cm^{-1} corresponds to N=C=S stretching vibrations
Alkene	medium band	1636cm^{-1} corresponds to C=C stretching vibrations
Amine	medium band	1108cm^{-1} corresponds to C-N stretching vibrations
Halo compound	strong band	669cm^{-1} corresponds to C-Br stretching vibrations

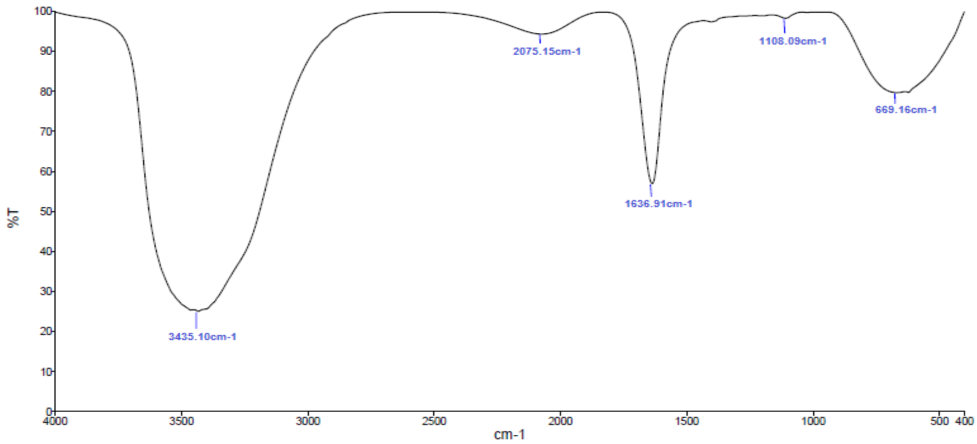

Figure 3. FTIR spectrum of synthesized silver nanoparticles using sample.

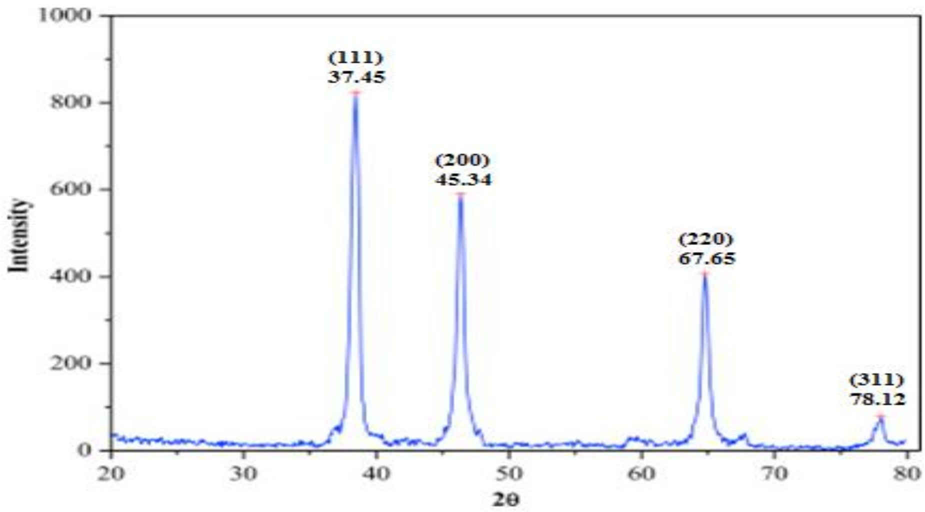

Figure 4. XRD Analysis of Synthesized Silver Nanoparticles Using Samplee**.**

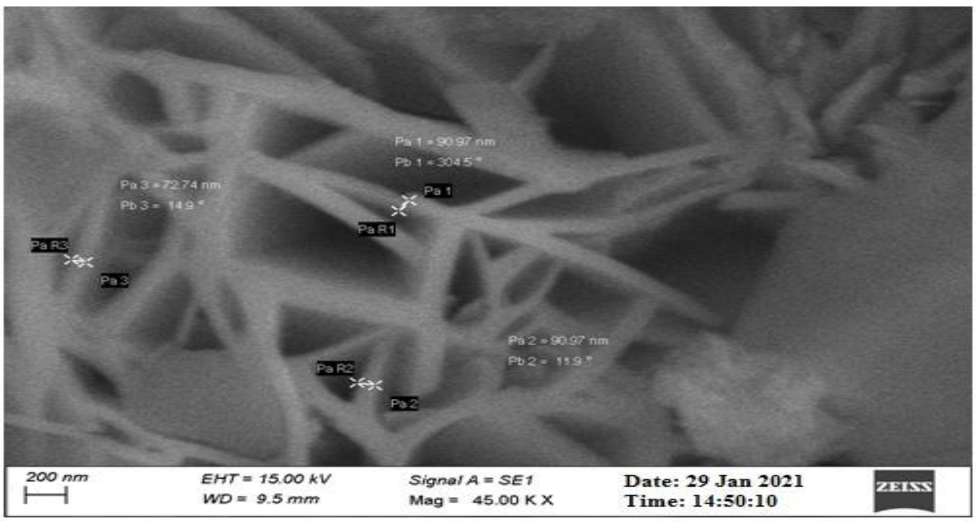

Figure 5. SEM photograph of synthesized silver nanoparticles using sample

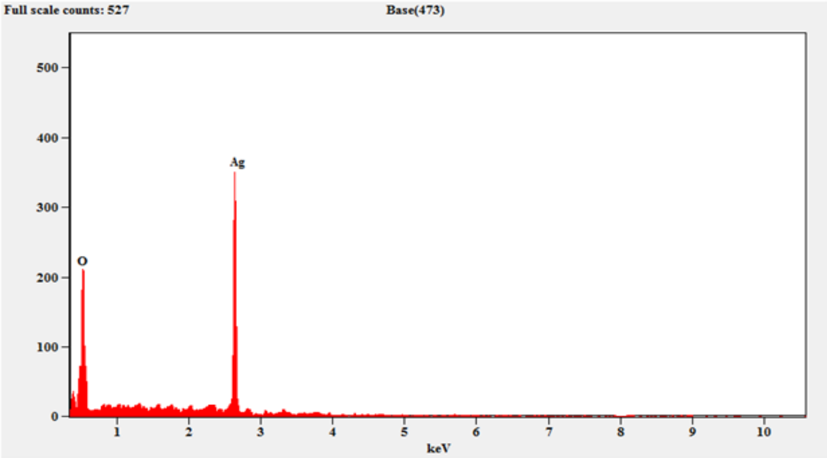

Figure 6. EDX spectrum of synthesized silver nanoparticles using sample.

Table 4. Elemental composition of synthesized silver nanoparticles

Element	Wt%	At%
O	35.19	77.29
Ag	64.81	22.21

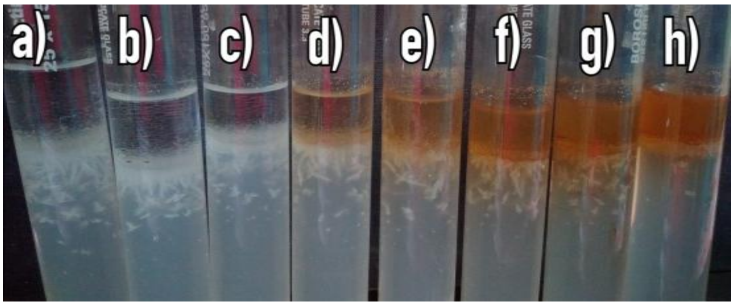

Figure 7. Growth of the struvite crystals.

Pure control, With distilled water, With ethanol, With 0.15% extracts, With 0.25% extracts, With 0.50% extracts, With 0.75% extracts, With 1.0% extract

Table 5. Harvested crystals percentage inhibition.

Crystal	Class	Analysis	Harvested crystals (gm)	Inhibition Percentage
	A	Control	2.46	0%
	B	Control +distilled water	2.12	13.8%
	C	Control + ethanol solution	1.48	39.8%
	D	Control + 1% synthesized silver nanoparticles	1.26	48.7%
Struvite	E	Control + 2% synthesized silver nanoparticles	0.85	65.4%
	F	Control + 3% synthesized silver nanoparticles	0.69	71.9%
	G	Control + 4% synthesized silver nanoparticles	0.47	80.8%
	H	Control + 5% synthesized silver nanoparticles	0.25	89.8%

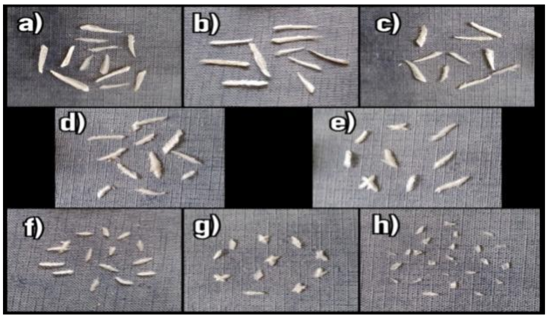

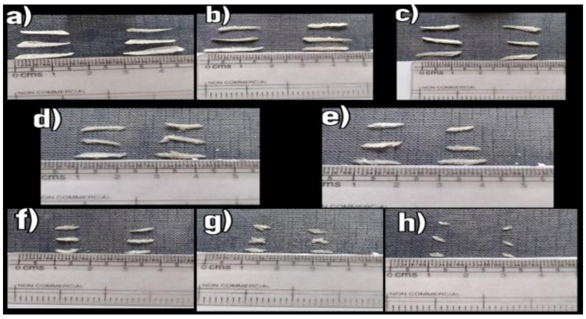

Figure 8. Morphology of harvested CHPD **Figure 9.** Scale measurement of harvested CHPD

(A) Pure control (B) distilled water (C) ethanol (D) 0.15% extracts (E)0.25% extracts (F) 0.50 % extracts (G) 0.75% extracts (h) 1.0% extracts

The FT-IR spectra of struvite crystals obtained in the presence and absence of the plant sample *(Brenia retusa* stem) are given in the Table 6 and Figure 10.

Table 6. The FT-IR spectra of struvite crystals.

Figure	Frequency cm-1	Functional group
Control A	2358	Anti symmetric and symmetric stretching Vibration of NH4 units
	1636	HOH deformation of water
	1440	HNH deformation of NH4 units
	1004	V3 antisymmetric stretching vibration
	758	Librational of water and NH4 rocking modes
	568	V4 bending modes of te PO4 unit

Figure	Frequency cm-1	Functional group
Control +5%	2374	Antisymmetic and symmetric stretching, vibration of NH4 units
	1600	HOH deformation of water
	1438	HNH deformation of modes of NH4 units
	1004	V3 antisymmetric stretching vibration
	758	Liberation of water and NH4 rocking modes
	568	V4 bending modes of the PO4 units

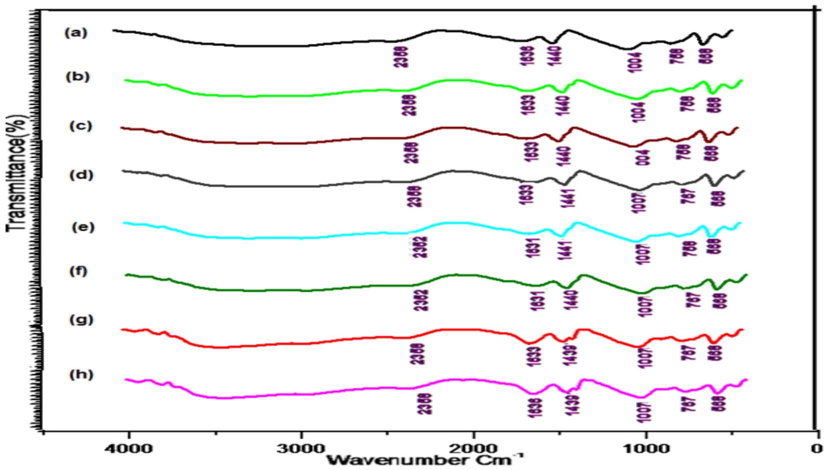

Figure 10. FT-IR of struvite crystals.

Some of the researcher said that characterization crystallization of struvite crytal FTIR techniques. The peaks move from 2358 to 2374 cm-1 antisymmetric, symmetric stretching and vibration of NH4 units and from 1440 to 1438 cm-1 for N-H deformation of modes of NH4 units already reported. The shifting additionally supports that the extract can further formation of ammonium magnesium phosphate crystals and them reduce the nucleation rate of struvite crystal. The present investigation confirms the successful green synthesis of silver nanoparticles (AgNPs) using *Breynia retusa* stem extract and demonstrates their notable antiurolithiatic efficacy. Phytochemical screening revealed the presence of important secondary metabolites, including tannins, phenols, flavonoids, and alkaloids, which are widely recognized for their dual role as reducing and stabilizing agents during nanoparticle formation. The relatively higher levels of tannins (0.128 mg/g) and phenols (0.02 mg/g) indicate a strong antioxidant potential, which may contribute to the suppression of crystal formation by neutralizing reactive species and interfering with nucleation processes. Comparable findings have shown that phenolic compounds can inhibit crystal aggregation by interacting with crystal surfaces (Pareta *et al*., 2012; Bashir & Gilani, 2009). The synthesis of AgNPs was validated through UV-Visible spectroscopy, which exhibited a distinct surface plasmon resonance peak at 467 nm, a characteristic feature of silver nanoparticles. This observation aligns with earlier reports on plant-mediated nanoparticle synthesis (Gurunathan *et al*., 2015).

FTIR analysis further supported the involvement of various functional groups such as amines, alkenes, and isothiocyanates, indicating that phytoconstituents actively participate in the reduction of silver ions and stabilization of the nanoparticles. X-ray diffraction patterns confirmed the crystalline nature of the particles, while scanning electron microscopy revealed predominantly spherical nanoparticles within the size range of 72-90 nm. These structural features are consistent with previously reported plant-derived AgNPs (Li *et al*., 2010).

Elemental analysis using EDX demonstrated a high proportion of silver (64.81%), confirming efficient conversion of silver ions into nanoparticles. Such high purity is often associated with enhanced biological performance, particularly in antimicrobial and crystal inhibition applications. The antiurolithiatic potential assessed through the gel diffusion method showed a clear concentration-dependent inhibition of struvite crystal growth. The untreated system exhibited maximum crystal formation, whereas nanoparticle-treated samples showed a significant reduction in crystal mass. The highest inhibitory effect (89.8%) observed at 5% concentration highlights the strong capacity of AgNPs to interfere with crystal growth dynamics. This effect may be attributed to the adsorption of nanoparticles onto active crystal growth sites, thereby preventing further deposition of ions and limiting crystal enlargement. Additionally, FTIR analysis of the harvested crystals revealed subtle shifts in spectral peaks, suggesting modifications in the chemical structure of the crystals and reduced formation of ammonium magnesium phosphate. These changes indicate that the nanoparticles disrupt crystallization pathways at a molecular level. Similar observations have been reported in studies involving plant extracts, where bioactive compounds alter crystal morphology and inhibit growth (Nagarajan *et al*., 2019).

CONCLUSION

In summary, *Breynia retusa*-mediated silver nanoparticles exhibit potent antiurolithiatic activity by targeting multiple stages of stone formation, including nucleation, growth, and aggregation. The synergistic interaction between phytochemicals and nanoscale properties enhances their overall therapeutic effectiveness, suggesting their potential as a sustainable and efficient alternative for managing urolithiasis.

ACKNOWLEDGMENT

The authors express sincere thanks to the head of the Department of Microbiology, EGS Pillay Arts and Science College, Nagapattinam, Tamil Nadu, India for the facilities provided to carry out this research work.

CONFLICT OF INTERESTS

The authors declare no conflict of interest

ETHICS APPROVAL

Not applicable

FUNDING

This study received no specific funding from public, commercial, or not-for-profit funding agencies.

AI TOOL DECLARATION

The authors declare that no AI and related tools are used to write the scientific content of this manuscript.

DATA AVAILABILITY

Data will be available on request

REFERENCES

Alelign, T., & Petros, B. (2018). Kidney stone disease: An update on current concepts. *Advances in Urology, 2018*, Article 3068365. doi:10.1155/2018/3068365.

Bashir, S., & Gilani, A. H. (2009). Antiurolithic effect of *Bergenia ligulata* rhizome: An explanation of the underlying mechanisms. *Journal of Ethnopharmacology, 122*(1), 106-116. doi: 10.1016/j.jep.2008.12.004.

Gurunathan, S., Han, J. W., Park, J. H., Kim, E., Choi, Y. J., Kwon, D. N., Kim, J. H., & Kim, J. H. (2015). Green synthesis of silver nanoparticles using plant extracts and their antimicrobial activities: A review. *International Journal of Nanomedicine, 10*, 4203-4217. doi:10.2147/IJN.S79579.

Hesse, A., Brändle, E., Wilbert, D., Köhrmann, K. U., & Alken, P. (2003). Study on the prevalence and incidence of urolithiasis in Germany comparing the years 1979 vs. 2000. *European Urology, 44*(6), 709-713. doi:10.1016/S0302-2838(03)00415-9.

Johri, N., Cooper, B., Robertson, W., Choong, S., Rickards, D., & Unwin, R. (2010). An update and practical guide to renal stone management. *Nephron Clinical Practice, 116*(3), c159-c171. doi:10.1159/000317196

Li, W. R., Xie, X. B., Shi, Q. S., Zeng, H. Y., Ou-Yang, Y. S., & Chen, Y. B. (2010). Antibacterial activity and mechanism of silver nanoparticles on *Escherichia coli*. *Applied Microbiology and Biotechnology, 85*(4), 1115-1122. doi:10.1007/s00253-009-2159-5.

Nagarajan, Y., Boopathi, R., Yahoob, S. A. M., & Venkatraman, A. (2019). In vitro evaluation of antiurolithiatic activity of *Bryophyllum pinnatum* Lam. *International Journal of Scientific Research in Multidisciplinary Studies, 5*(8), 97-102.

Pareta, S. K., Patra, K. C., Mazumder, P. M., & Sasmal, D. (2012). Establishing the principle of herbal therapy for antiurolithiatic activity: A review. *Journal of Pharmacology and Toxicology, 7*(1), 1-12. doi:10.3923/jpt.2012.1.12.

Stamatelou, K. K., Francis, M. E., Jones, C. A., Nyberg, L. M., & Curhan, G. C. (2003). Time trends in reported prevalence of kidney stones in the United States: 1976-1994. *Kidney International, 63*(5), 1817-1823. doi:10.1046/j.1523-1755.2003. 00917.x.